Optically In-Well-Pumped Semiconductor Disk Laser With Low Quantum Defect

Alexander Hein and Uwe Brauch *

An in-well pumped InGaAs disk laser emitting at 984 nm is presented. The device is designed to eliminate major loss mechanisms attributed to heat generation in semiconductor disk lasers. An output power of close to 7 W at room temperature is achieved by optical excitation with a fiber-coupled 940 nm diode laser. Strong cooling or the use of heat spreaders with high thermal conductivity is not necessary. For the investigated pump levels, absorptance values of 48 % are realized without pump recycling. The optical output shows no indication of thermal rollover at room temperature, but is limited by the currently available pump power.

1. Introduction

Generating output powers in optically pumped semiconductor disk lasers (OPSDLs) beyond 10 W is essentially possible due to rather strong cooling [1, 2], partially with liquid nitrogen [3], and the use of high thermal conductivity diamond heat spreaders with mm-scale thickness [4, 5]. Another alternative to diminish the temperature rise in the active region is to attach an optically transparent single-crystal diamond or SiC intra-cavity heat spreader on the front face of the semiconductor disk to bypass the thermal resistance of the highly reflective distributed Bragg reflector (DBR) layers on the backside [6–8]. In endorsement of the cited works it should be noted that for a straightforward and ingenuous comparison of OPSDL performance, it is not sufficient to simply relate output power, but more ratios or factors like output power/spot size, coolant temperature/sample temperature, quantum defect, etc. have to be accounted for. However, room temperature operation with an output power of greater than 10 W to date was never reported for devices that are not based on strong cooling or high thermal conductivity heat spreading materials. OPSDLs with output powers beyond 20 W are typically found in the spectral region 980–1180 nm, drawing on the advantages of strained InGaAs quantum wells (QWs) and good carrier confinement with GaAs/GaAsP/AlGaAs barriers. These devices are mostly pumped with high-power 808 nm laser diodes, where the main part of the pump radiation is being absorbed in the barriers surrounding the QWs due to the high absorption coefficient in these materials at the described pump wavelength of ten to few thousand per cm. The advantage is a short absorption depth allowing for designs of thin active regions and single-pass pumping. However, two major disadvantages arise: a relatively large quantum defect (20–35 %) for 980–1180 nm emission and an inhomogeneous carrier distribution in

* Uwe Brauch is with the IFSW (Institut für Strahlwerkzeuge), Universität Stuttgart, Germany

the respective QWs resulting in increased threshold pump powers [9]. Contrary, in in-well pumped (IP) semiconductor disk lasers, the quantum defect can be essentially minimized to about 5 % for the laser structure described here, thus being comparable to or even lower than in Yb:YAG laser systems. Considering the overall system performance, the efficiency of strained InGaAs-QW based pump diodes emitting above 900 nm is by about 5–10 % higher than unstrained AlGaAs/GaAs-QW based diodes, typical for the spectral emission range of 800–850 nm. Moreover, the implementation of fully binary compound (AlAs/GaAs) mirrors does not suffer from absorption of the remaining pump radiation, thus not contributing to the heat load in the device. Calculations in [10] reveal that the quantum defect and pump absorption in the mirror are responsible for roughly 40 % of loss in output power with similar contributions for an OPSDL pumped at 808 nm and an emission around 1025 nm. According to simulations in [11] disadvantages for in-well pumped structures may arise from gain reduction at the lasing energy due to kinetic hole burning and reduction of the pump absorption due to Pauli blocking. However, since efficient IP structures [12] often utilize a top Bragg reflector in order to resonantly increase the absorption, the modal gain for the emission wavelength is also increased as a consequence of the spectral proximity of the laser and pump resonance, thus counteracting both mentioned shortcomings.

2. Laser Design and Setup

The presented structures are grown in reverse order, top mirror—active region—bottom mirror, by molecular beam epitaxy (MBE) on n-doped 350 µm thick GaAs substrates with (100) orientation. The active region consists of two identical resonant periodically arranged QW packages separated by a GaAs spacer. Each QW package contains 4 periods of double $In_{0.16}Ga_{0.84}As$ QWs that are compressively strained. The active region was grown at a reduced thermocouple substrate temperature of 420°C to prevent indium diffusion while a typical growth temperature for the DBRs is 480°C. Similar to the work described in [13] strain compensation of the QWs is achieved by placing tensilely strained GaAsP layers into the barriers separating the QWs. The GaAs spacer is needed to account for the dephasing of the optical field intensities of the emission and the pump wavelength since pump absorption can only take place in the QW and hence, its antinodes need to overlap with the emission field pattern. The top and bottom Bragg reflectors were realized by a 3.5 and a 24.5 pair AlAs/GaAs sequence, respectively, the reflectivity of the latter further increased by a Ti/Au metalization evaporated directly onto the epitaxial surface, providing a reflectivity of > 99.95 % at the center wavelength.

The metalized structures are soldered with indium onto gold-plated copper heat sinks and the substrate is removed via wet-chemical etching. The laser samples are completed with a tantalum pentoxide (Ta_2O_5) coating applied by ion beam sputter deposition. By this, the semiconductor surface (GaAs) with its potentially absorbing surface states can be placed in a node of the laser field. The structure design is depicted in Fig. 1. The pump light is assumed to be unpolarized and regarding the distribution of the pump field intensity there is almost no difference between the TE- and TM-component, so that only the TE-component is displayed.

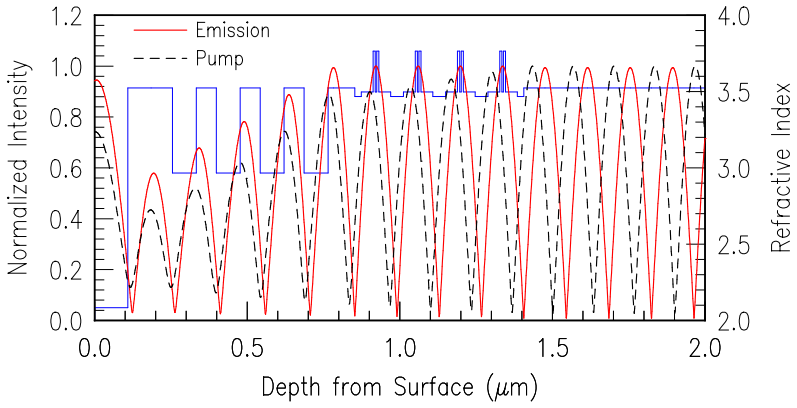

Fig. 1: Refractive index representation of the designed structure and field intensities of the emission and pump (TE-component) wavelength. Displayed is the dielectric coating (Ta_2O_5, $\bar{n} = 2.08$), the top reflector, and the first half of the active region.

Figure 2 shows the measured surface reflectivities for different angles of incidence. Near normal incidence (10° was the smallest possible angle) three dips can be identified within the stop band of the DBR which extends from 925 to 1025 nm. While the excitonic dip at 970 nm remains unchanged with varying angle, the sub-cavity resonances experience the typical cosine shift to shorter wavelengths with an increasing angle of incidence. At 10° the pump and emission resonance are found at 954 nm and 993 nm, respectively, while the latter becomes more pronounced for larger angles as a consequence of a better overlap with the excitonic dip. The detuning between exciton and emission resonance at normal incidence is roughly 24 nm and should promote operation at higher temperatures. The spectral position of the pump resonance follows the same cosine dependence, while the absorption strength shows a linear reduction (increase in reflectivity from 10 % to 20 %) for

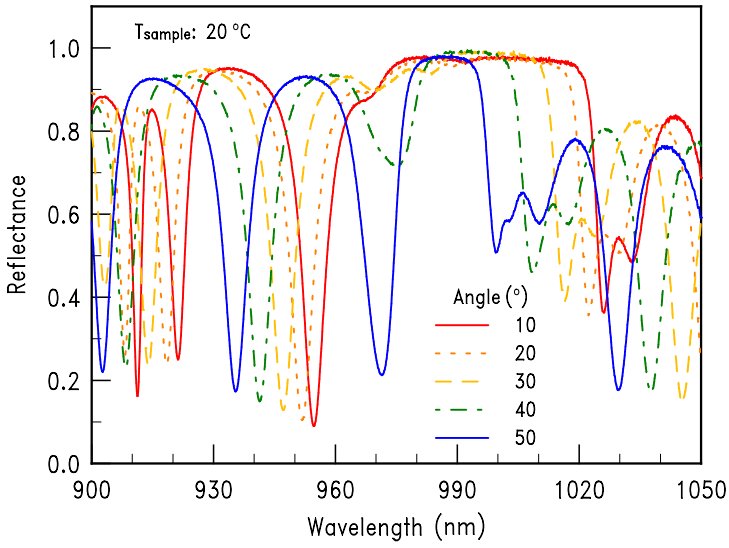

Fig. 2: Reflectivity spectra with varying angles of incidence. Both, laser and pump resonance are visible as pronounced dips in reflector's stop band.

the indicated angles. For pumping with 940 nm diodes and accounting for the temperature dependent spectral shift, the optimum pump angles for a high absorption efficiency are found in the range of 30°–40°.

To characterize the lasing parameters the structures under test were pumped with a fiber-coupled laser diode emitting between 930 and 940 nm depending on the pump current with a maximum output power of roughly 40 W. The beam was focused onto the samples at angles of 24°–26° to give a slightly elliptical spot of $370 \times 420\,\mu m^2$ in the y- and x-axis, respectively. The copper heat sinks were cooled by water of 15°–20°C. A linear resonator with a concave output coupler of −150 mm radius of curvature and transmittance of 2.8 % was used to perform the lasing experiments.

3. Results and Discussion

For high-power operation, care has to be taken to maximize the absorption efficiency of the pump power at the point of operation, e. g., at maximum pump power. This strongly depends on the wavelength of the free-running pump diodes (which is a function of the operating current and cooling-water temperature), the angle of incidence, the temperature of the active region of the disk (which is a function of the absorbed pump power, the heat-sink temperature, and possibly the laser efficiency), and the laser threshold (which is a function of the active-region temperature and the resonator losses, including the outcoupling losses). An example of the absorption efficiency as function of the incident pump power is shown in Fig. 3 for two different devices.

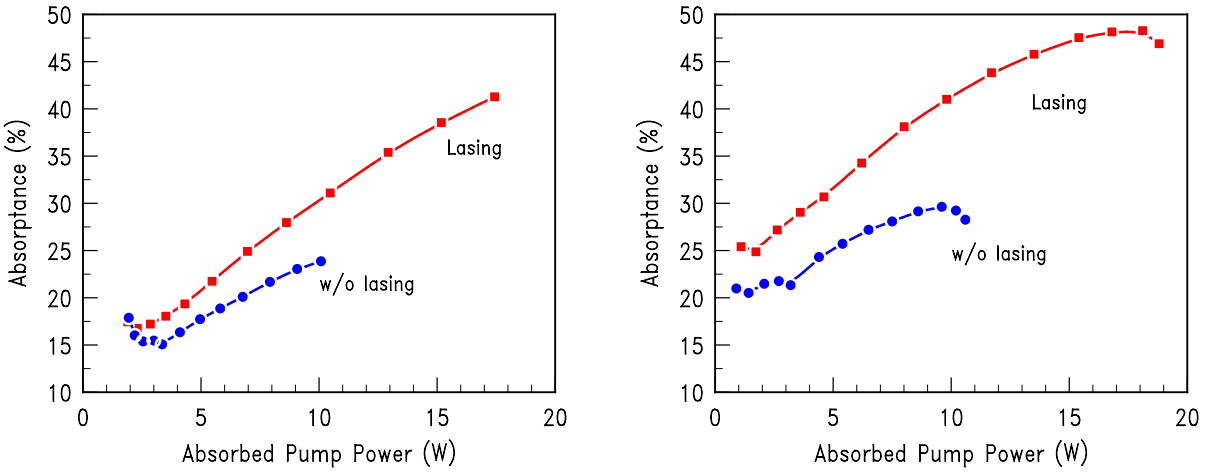

Fig. 3: Absorption efficiency of the pump radiation as function of the incident pump power for two cases: lasing with 2.8 % out-coupling (squares) and not lasing (circles) with out-coupling for two different lasers (left and right).

The absorption increase is mainly due to the shift of the diode laser wavelength into the cavity resonance. The absorption efficiency does not reach the value of 80–90 % one might have expected from the reflectance spectra. This is because with higher population of the upper laser level the wavelength for which the sample is transparent — i.e., the

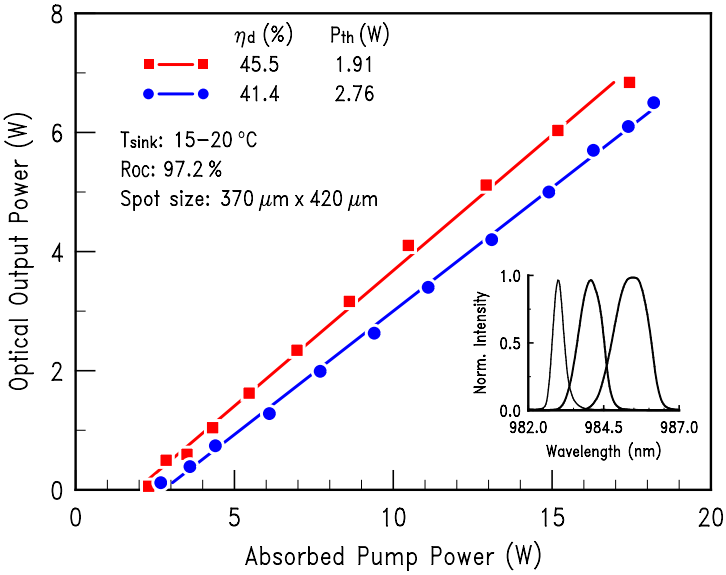

Fig. 4: Laser output power versus absorbed pump power for two devices. The inset shows optical spectra for different excitation levels.

transition from the gain to the absorption region — moves more and more towards shorter wavelengths and finally approaches the pump wavelength. The increase in bleaching is not expected above the lasing threshold where the inversion should be clamped at the threshold value. However, because of heating and other effects this is not strictly true, but the population, and consequently the bleaching, grows significantly slower than under the non-lasing conditions. Laser output power versus absorbed pump power is shown in Fig. 4. The threshold pump power of 2 W corresponds to a power density of 600 W/cm^2, being within a typical range for OPSDLs. The maximum output power, which is limited by the available pump power, is close to 7 W for both devices. The slope efficiency of 45 % is comparable to values typically obtained in barrier pumped structures, but is believed to be limited by the currently relatively poor epitaxial quality of the laser material. The locally resolved photoluminesce of a laser disk is depicted in Fig. 5, where the internal defects can be seen.

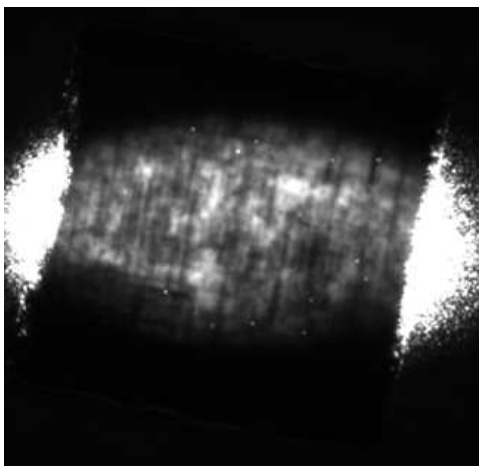

Fig. 5: Locally resolved photoluminescence image of a laser chip. The chip size is approximately $2 \times 2\,\mathrm{mm}^2$. The sample was illuminated with the pump laser diode emitting at 940 nm.

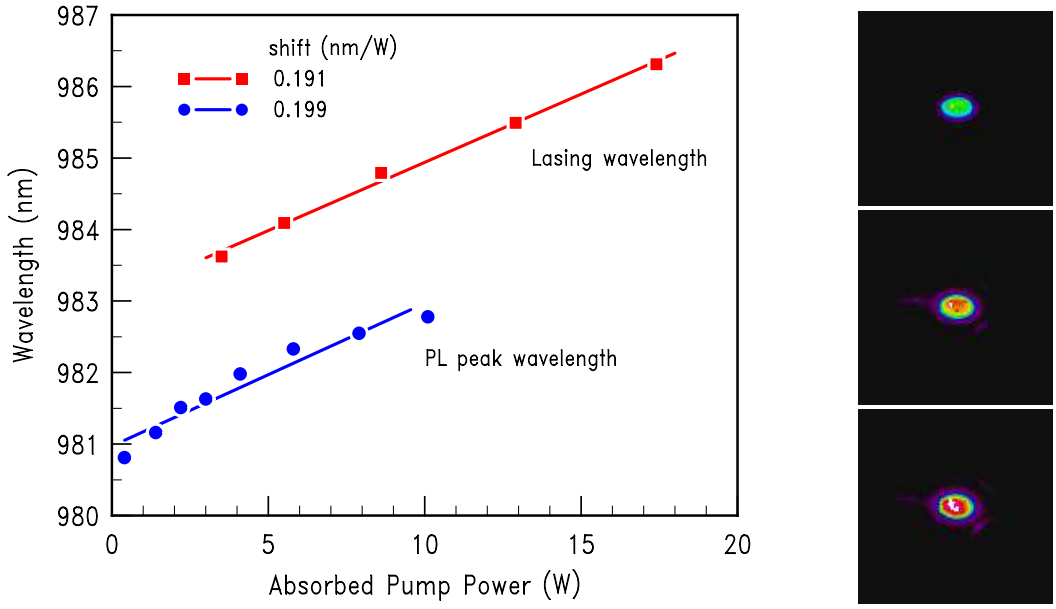

Fig. 6: Lasing wavelength and photoluminecsence wavelength shifts (without outcoupling mirror) versus absorbed pump power (left). Pump spots at different levels of the absorbed pump power (top: 3 W, center: 5.8 W, bottom: 10.1 W) during the PL measurements (right).

Main disadvantage for these devices is the reduced pump absorption. Chosen here was a compromise between absorption efficiency on the one hand and tolerance against misalignment on the other hand. A measured reflectance of roughly 20 % in non-lasing conditions allows to get almost half of the pump power (48 %) been absorbed in one double-pass. With a second double-pass (retro-reflection) one should already get a sufficiently high absorption efficiency (75 %) to realize higher optical outputs. With even more sophisticated pumping schemes, by the use of multipass pump optics, absorptance values comparable to barrier pumped devices (> 90 %) could be easily realized. The in-well pumping scheme allows to operate the laser with almost no sign of thermal rollover despite the relatively simple cooling setup. Using more efficient cooling schemes like diamond heat spreaders should allow to achieve much higher output powers and possibly the regime where a one-dimensional heat flow is sufficient for cooling. This would allow to scale the optical output power freely with the pump-spot size. The results shown here have been achieved with standard diodes without any wavelength stabilization and neither the cooling water for the diodes nor for the laser disk has been stabilized either. Adding volume Bragg gratings (VBGs) to the pump diodes for wavelength stabilization and a temperature controller for the cooling water should further increase the stability of the pump absorption and may even allow to increase the resonance to further enhance the absorption efficiency of one double pass.

The laser wavelength shows a red-shift towards longer wavelengths with 0.191 nm/W; the PL wavelength (without lasing) shifts slightly stronger with 0.199 nm/W absorbed power as depicted in Fig. 6. With a tyical shift of the DBR resonance of 0.07 nm/K this corresponds to a heating of the active layer of 2.73 K/W and 2.84 K/W.

4. Conclusion

In summary, in-well pumped disk lasers emitting at a wavelength of 984 nm with an output power close to 7 W have been demonstrated. The optical output power for this particular type of disk laser is believed to be the highest obtained so far. Thermal rollover is not observed although at maximum output power the laser operates at 9 times of the threshold power while only a simple cooling setup is used. It is likely that with these devices a one-dimensional heat-flow regime may be sufficient for cooling, thus, true power scaling with increasing the pump spot size can become feasible.

Acknowledgment

The authors would like to thank Susanne Menzel for the epitaxial growth of the laser material and Rudolf Rösch for his support with chip processing and mechanical issues.

References

[1] F. Demaria, S. Lorch, S. Menzel, M.C. Riedl, F. Rinaldi, R. Rösch, and P. Unger, "Design of highly efficient high-power optically pumped semiconductor disk lasers", *IEEE J. Select. Topics Quantum Electron.*, vol. 15, pp. 973–977, 2009.

[2] B. Rudin, A. Rutz, M. Hoffman, D.J.H.C. Maas, J.-R. Bellancourt, E. Gini, T. Südmeyer, and U. Keller, "Highly efficient optically pumped vertical-emitting semiconductor laser with more than 20 W average output power in a fundamental transverse mode", *Opt. Lett.*, vol. 33, pp. 2719–2721, 2008.

[3] A. Chernikov, J. Herrmann, M. Koch, B. Kunert W. Stolz, S. Chatterjee, S.W. Koch, T.-L. Wang, Y. Kaneda, J.M. Yarborough, J. Hader, and J.V. Moloney, "Heat management in high-power vertical-external-cavity surface emitting lasers", *IEEE J. Select. Topics Quantum Electron.*, vol. 17, pp. 1772–1778, 2011.

[4] P. Unger, A. Hein, F. Demaria, S. Menzel, M. Rampp, and A. Ziegler, "Design of high-efficiency semiconductor disk lasers", in *Vertical External Cavity Surface Emitting Lasers (VECSELs) III*, J.E. Hastie (Ed.), Proc. SPIE 8606, pp. 860602-1–8, 2013.

[5] B. Heinen, T.-L. Wang, M. Sparenberg, A. Weber, B. Kunert, J. Hader, S.W. Koch, J.V. Moloney, M. Koch, and W. Stolz, "106 W continuous-wave output power from vertical-external-cavity surface-emitting laser", *Electron. Lett.*, vol. 48, pp. 516–517, 2012.

[6] K.-S. Kim, J. Yoo, G. Kim, S. Lee, S. Cho, J. Kim, T. Kim, and Y. Park, "Enhancement of pumping efficiency in a vertical-external-cavity surface-emitting laser", *IEEE Photon. Technol. Lett.*, vol. 19, pp. 1925–1927, 2007.

[7] S. Ranta, M. Tavast, T. Leinonen, N. Van Lieu, G. Fetzer, and M. Guina, "1180 nm VECSEL with output power beyond 20 W", *Electron. Lett.*, vol. 49, pp. 59–60, 2013.

[8] N. Schulz, S. Rösener, R. Moser, M. Rattunde, C. Manz, K. Köhler, and J. Wagner, "An improved active region concept for highly efficient GaSb-based optically in-well pumped vertical-external-cavity surface-emitting lasers", *Appl. Phys. Lett.*, vol. 93, pp. 181113-1–3, 2008.

[9] O. Casel, *Experimentelle Untersuchung und Modellierung des Einflusses der Epitaxiestruktur auf die physikalischen Eigenschaften optisch angeregter Halbleiterscheibenlaser*. Ph.D. Thesis, Technische Universität Kaiserslautern, Germany, 2005.

[10] J. Hader, T.-L. Wang, J.V. Moloney, B. Heinen, M. Koch, S.W. Koch, B. Kunert, and W. Stolz, "On the measurement of the thermal impedance in vertical-external-cavity surface-emitting lasers", *J. Appl. Phys.*, vol. 113, pp. 153102-1–4, 2013.

[11] E. Kühn, S.W. Koch, A. Thränhardt, J. Hader, and J.V. Moloney, "Microscopic simulation of nonequilibrium features in quantum-well pumped semiconductor disk lasers", *Appl. Phys. Lett.*, vol. 96, pp. 051116-1–3, 2010.

[12] S.S. Beyertt, U. Brauch, F. Demaria, N. Dhidah, A. Giesen, C. Kübler, S. Lorch, F. Rinaldi, and P. Unger, "Efficient gallium-arsenide disk laser", *IEEE J. Select. Topics Quantum Electron.*, vol. 43, pp. 869–875, 2007.

[13] A. Hein, S. Menzel, and P. Unger, "High-power high-efficiency optically pumped semiconductor disk lasers in the green spectral region with a broad tuning range", *Appl. Phys. Lett.*, vol. 101, pp. 111109-1–4, 2012.